

SANDIA REPORT

SAND2008-6080

Unlimited Release

Printed September 2008

Remotely Interrogated Passive Polarizing Dosimeter

Robert R. Boye, Cody M. Washburn, Sally Samora, Shanalyn A. Kemme, David R. Wheeler, Shawn M. Dirk, Daniel L. Buller

Prepared by
Sandia National Laboratories
Albuquerque, New Mexico 87185 and Livermore, California 94550

Sandia is a multiprogram laboratory operated by Sandia Corporation,
a Lockheed Martin Company, for the United States Department of Energy's
National Nuclear Security Administration under Contract DE-AC04-94AL85000.

Approved for public release; further dissemination unlimited.

Issued by Sandia National Laboratories, operated for the United States Department of Energy by Sandia Corporation.

NOTICE: This report was prepared as an account of work sponsored by an agency of the United States Government. Neither the United States Government, nor any agency thereof, nor any of their employees, nor any of their contractors, subcontractors, or their employees, make any warranty, express or implied, or assume any legal liability or responsibility for the accuracy, completeness, or usefulness of any information, apparatus, product, or process disclosed, or represent that its use would not infringe privately owned rights. Reference herein to any specific commercial product, process, or service by trade name, trademark, manufacturer, or otherwise, does not necessarily constitute or imply its endorsement, recommendation, or favoring by the United States Government, any agency thereof, or any of their contractors or subcontractors. The views and opinions expressed herein do not necessarily state or reflect those of the United States Government, any agency thereof, or any of their contractors.

Printed in the United States of America. This report has been reproduced directly from the best available copy.

Available to DOE and DOE contractors from
U.S. Department of Energy
Office of Scientific and Technical Information
P.O. Box 62
Oak Ridge, TN 37831

Telephone: (865) 576-8401
Facsimile: (865) 576-5728
E-Mail: reports@adonis.osti.gov
Online ordering: <http://www.osti.gov/bridge>

Available to the public from
U.S. Department of Commerce
National Technical Information Service
5285 Port Royal Rd.
Springfield, VA 22161

Telephone: (800) 553-6847
Facsimile: (703) 605-6900
E-Mail: orders@ntis.fedworld.gov
Online order: <http://www.ntis.gov/help/ordermethods.asp?loc=7-4-0#online>



Remotely Interrogated Passive Polarizing Dosimeter (RIPPeD)

Robert R. Boye, Sally Samora, Shanalyn A. Kemme
Photonic Microsystems Technologies

Cody M. Washburn, Shawn M. Dirk
Organic Materials

David R. Wheeler
Biosensors and Nanomaterials

Daniel L. Buller
Radiation-Solid Interactions

Sandia National Laboratories
PO Box 5800
Albuquerque, NM 87185-1082

Abstract

Conductive polymers have become an extremely useful class of materials for many optical applications. We have developed an electrochemical growth method for depositing highly conductive (~ 100 S/cm) polypyrrole. Additionally, we have adapted advanced fabrication methods for use with the polypyrrole resulting in gratings with submicron features. This conductive polymer micro-wire grid provides an optical polarizer with unique properties. When the polymer is exposed to ionizing radiation, its conductivity is affected and the polarization properties of the device, specifically the extinction ratio, change in a corresponding manner. This change in polarization properties can be determined by optically interrogating the device, possibly from a remote location. The result is a passive radiation-sensitive sensor with very low optical visibility. The ability to interrogate the device from a safe standoff distance provides a device useful in potentially dangerous environments. Also, the passive nature of the device make it applicable in applications where external power is not available. We will review the polymer deposition, fabrication methods and device design and modeling. The characterization of the polymer's sensitivity to ionizing radiation and optical testing of infrared polarizers before and after irradiation will also be presented. These experimental results will highlight the usefulness of the conductive infrared polarizer to many security and monitoring applications.

Table of Contents

Table of Contents	5
1. INTRODUCTION	7
2. DEVICE DESIGN	7
3. DEPOSITION OF CONDUCTIVE POLYMER.....	9
4. PHOTOLITHOGRAPHIC DEVICE FABRICATION	11
5. OPTICAL DEVICE CHARACTERIZATION.....	13
6. IONIZING RADIATION SENSITIVITY	15
7. CONCLUSIONS AND FUTURE WORK	19
8. REFERENCES	19

Figures

<i>Figure 1. Design and scanning electron micrograph of gold based wiregrid polarizer.</i>	<i>8</i>
<i>Figure 2. TM transmission and extinction ratio (ER) of gold and conductive polymer</i>	<i>9</i>
<i>Figure 3. The importance of the polymer conductivity and depth on the extinction</i>	<i>9</i>
<i>Figure 4. SEM images of spin coated PEDOT after lithographic processing.....</i>	<i>10</i>
<i>Figure 5. Schematic and original electrochemical cell built for polymer growth.....</i>	<i>11</i>
<i>Figure 6. Successfully patterned PPy films. Test etch of a relatively large feature</i>	<i>12</i>
<i>Figure 7. SEM image of transferred polymer grating embedded in Norland 61™.</i>	<i>13</i>
<i>Figure 8. Wafers showing (left to right) patterned photoresist, etched devices and</i>	<i>13</i>
<i>Figure 9. Optical test setup for characterizing optical devices. HeNe laser is on</i>	<i>14</i>
<i>Figure 10. Measured transmission of conductive polymer wire grid (dots) and.....</i>	<i>15</i>
<i>Figure 11. Measured data (dots) and simulated transmission (solid line) of polymer.....</i>	<i>16</i>
<i>Figure 12. Change of polymer conductivity with total dose. Results below 1Mrad.....</i>	<i>17</i>
<i>Figure 13. Modeled change in signal contrast of polymer polarizer based tag with</i>	<i>18</i>
<i>Figure 14. Optical response of device before and after exposure to 250keV protons.....</i>	<i>18</i>

1. INTRODUCTION

Electrically conducting polymers are an active area of research with optical applications ranging from photodetectors¹ and photovoltaic cells² to light emitting diodes³⁻⁵. Here we report on the development of a subwavelength grating utilizing conductive polymer. This device will have polarization dependent transmission and reflection characteristics due to the conductivity of the polymer. Various types of radiation, e.g. protons or X-rays, affect the conductivity of many polymers. A change in conductivity would have a corresponding effect on the optical performance of the device, particularly the polarization dependent properties. This sensitivity to ionizing radiation makes these devices applicable to the complex problem of detecting and monitoring such radiation from a remote location or large standoff distance. The main difficulty with detecting ionizing radiation from a distance is the rapid decrease in signal as the range from the source increases. Assuming the source is radiating in an isotropic fashion, the available signal will decrease as the square of the distance. A dosimeter that actively relays its information (e.g. electronically) would provide a remote monitoring method, but for many applications this device is too bulky, dependent on an adequate power source and easily defeated. A passive device like an optical polarizer is much more innocuous and can be interrogated either passively or actively from a large distance.

Rigorous coupled wave analysis (RCWA) of the basic device structure provided design targets for the fabrication. The next section reviews the results of this modeling effort highlighting the contrasts between a micro-wiregrid polarizer based on a metallic grating and a conductive polymer based device. The polymer deposition development is reviewed in Section 3 and covers the original spin coating work as well as the more successful electrochemical deposition. Section 4 will review the device fabrication process and Section 5 will discuss the optical characterization of several devices. The effects of ionizing radiation on the device optical performance will be discussed in Section 6.

2. DEVICE DESIGN

The key to these applications is a polarizer with an extinction ratio dependent on the absorbed dose of ionizing radiation. A brief review of wire grid polarizers will help illustrate the use of conducting polymers and the development of the device. In the most basic sense, a wire grid polarizer is a set of conducting lines that absorbs incident optical radiation that is oriented along the lines while passing optical radiation that is polarized in a perpendicular orientation⁶⁻⁸. Figure 1 shows the details of a wire grid device previously fabricated for the MWIR (2-5 μm) spectral range⁶. This device used gold as the conducting material and a subwavelength grating period to provide an extinction ratio greater than 100 with high transmission. The approach for this project is to replace the gold with a conductive polymer.

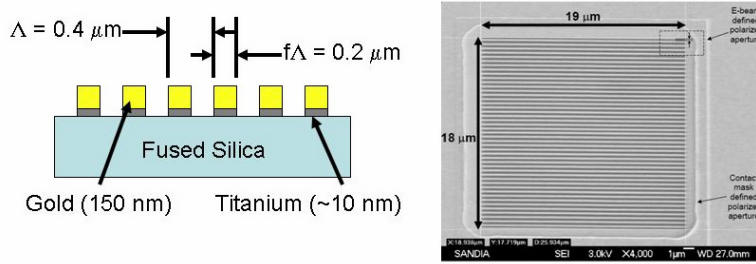


Figure 1. Design and scanning electron micrograph of gold based wiregrid polarizer.

The conductive polymer used here is polypyrrole. Published values for the refractive index of pyrrole vary from 1.505 to 1.8⁹⁻¹⁰. The imaginary part of the refractive index can be estimated from the conductivity of the polymer. Doped polymers can have conductivities, σ , as high as 100 S/cm¹¹⁻¹². The imaginary index can be found from¹³:

$$nk = \frac{2\pi\mu\sigma}{\omega} \quad (1)$$

Where n is the real part of the refractive index, k is the imaginary part, μ is the permeability and ω is the frequency. It is important to note that these values are dependent on several factors including the synthesis method used and the level of doping required to achieve the desired conductivity. Using a refractive index of 1.5 and conductivity of 100 S/cm, the imaginary part of the refractive index for a wavelength of 3.39 μm is 0.667. A comparison of the simulated performance of the gold based polarizer from Figure 1 and the same grating using a conductive polymer is shown in Figure 2. The gold based wire grid needs a small thickness to achieve a large extinction ratio while also providing a high transmission of the passed polarization. In contrast, conductive polymer ($\sigma = 100$ S/cm) requires a much higher thickness to achieve a good extinction ratio. Unfortunately, the transmission of the polymer based polarizer is adversely effected by the thicker material. This result highlights the need to provide a polymer with as high a conductivity as possible. Additionally, the device fabrication must not reduce this conductivity while producing a grating with much higher aspect ratios (height versus width of line) than the gold based device.

Once a polarizer is successfully fabricated, its sensitivity to radiation determines its performance. The dependence of the polarizer extinction ratio to the conductivity of the material is shown in Figure 3. As the conductivity of the material decreases, the extinction ratio also declines rapidly. This change in extinction ratio is the measured parameter that is used to determine the radiation dose the device has received.

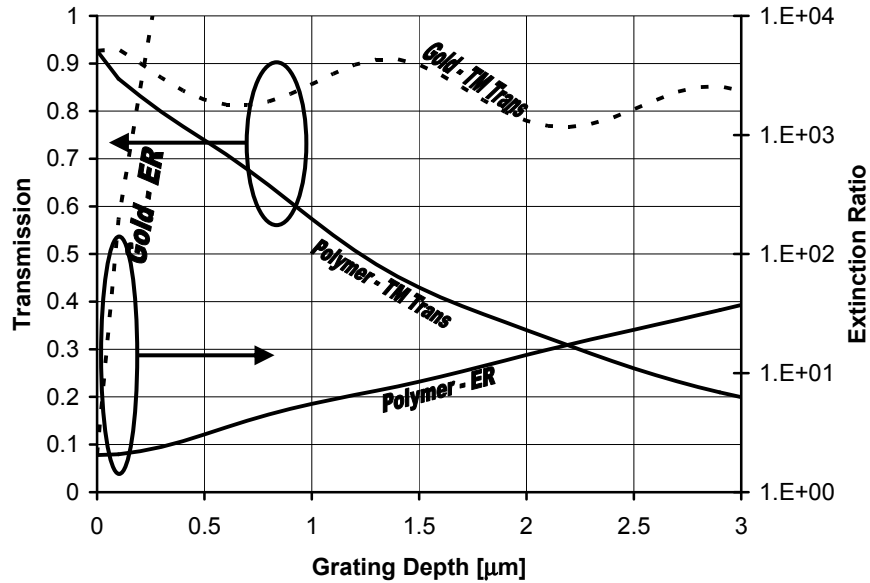


Figure 2. TM transmission and extinction ratio (ER) of gold and conductive polymer based IR polarizers versus grating depth. The polarizers were modeled with a fused silica substrate, $\Lambda = 0.4 \mu\text{m}$, $f = 0.5$ and $\lambda = 3.39 \mu\text{m}$.

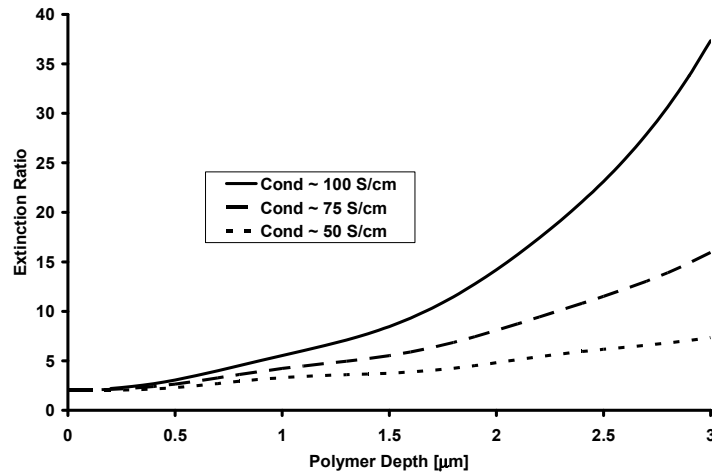


Figure 3. The importance of the polymer conductivity and depth on the extinction ratio of the polarizer.

3. DEPOSITION OF CONDUCTIVE POLYMER

The first deposition approach used was spin coating. Creating a film of polymer from solution using a spinner is a straightforward process that has been used successfully to create films with good uniformity and conductivity^{1,2,5,11,12,14,16,17}. Unfortunately, a single spin coated film has a thickness on the order of 100 nm. This thickness can be varied by changing the solution and spin recipe; however, to achieve the thickness required for a polarizer, multiple coatings will be needed. The material used was a commercial formulation of PEDOT [poly(3,4-ethylenedioxythiophene) poly(styrene sulfonate)] (“Baytron P” from H.C. Stark¹⁸). The solution was thinned with ethanol to help the coating uniformity and wetting. Ethylene glycol and NMP

were also tried as solvents, but these solutions did not wet to the substrate as well. A PEDOT:ethanol (2:1) mixture was filtered with a syringe filter and resulted in a coating thickness of approximately 100 nm with a top spin speed of 4000 rpm. Due to the rapid evaporation of ethanol, the substrates were immediately baked on a hot plate between 90 and 100 °C. Higher temperatures tended to cause the film to delaminate. The dwell time for this bake increased for each successive layer. Films were made with 3 or 4 layers and had thicknesses up to 500 nm with conductivities reaching a maximum of 100 S/cm.

Unfortunately, these films did not prove robust enough for photolithographic processing. Adhesion of the film to the substrate was often poor and the polymer was removed with common solvents such as acetone. The addition of a protective overcoat of polystyrene did allow for the application and patterning of photoresist. Gratings with features as small as 600 nm were successfully patterned in the photoresist; however, the etch selectivity was poor and the patterns were not successfully transferred to the polymer film. SEM images of the processed film show some of the resulting features, see Figure 4. In Figure 4a, an etched polymer film shows trenches that did not clear during the etch process. Figure 4b shows the graininess of 0.6 μm lines due to the large particulate size from the polymer solution. Finally, Figure 4c shows that the layer to layer adhesion of the multiple spin coats was often inconsistent. Portions of the top layer have broken and shifted independently of underlying layers.

Since the ultimate goal is to create submicron features, the large particulate size of the spin coated conductive polymer does not appear to be a compatible processing path. With the difficulties of adhesion and process stability already mentioned, this approach was not pursued further.

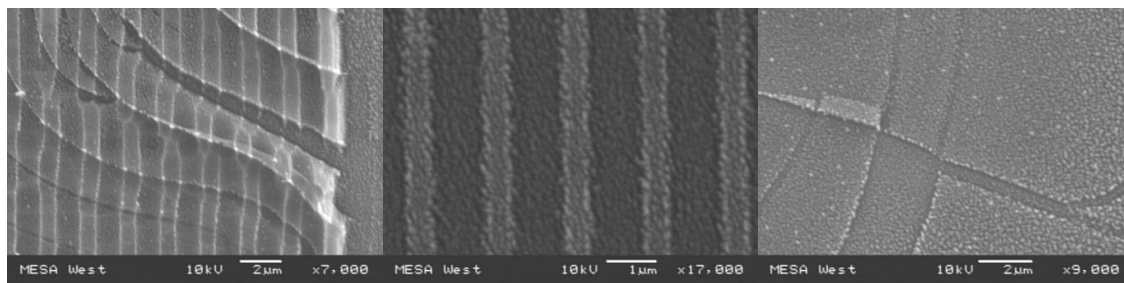


Figure 4. SEM images of spin coated PEDOT after lithographic processing. The etch selectivity between photoresist and polymer resulted in gratings without the trenches cleared (left). The graininess of the polymer was visible with the small lines being fabricated (center) and the adhesion between layers proved to be inconsistent (right).

Previous work on conductive polymers for optical applications has typically used one of three material systems: aniline^{12,14-15}, thiophene¹⁶⁻¹⁸ (used in spin coating work) or pyrrole^{9-10,19-21}. In addition to the spin coating effort, our work has used electrochemically deposited polypyrrole, doped to provide high conductivity. This approach provided material with high conductivity that was environmentally stable and also able to be processed lithographically.

Polypyrrole films were grown on fused silica and gallium arsenide substrates that had a thin titanium (25 nm) / gold (30 nm) coating. The substrates were first prepared using a silver substitution in a three-electrode electrochemical cell, see Figure 5, to help adhesion of the polymer film²². The deposition and gold oxidation phase take place on the auxiliary electrode of

the electrochemical cell while the working electrode has repeated use for each additional substrate used on the auxiliary electrode. Subsequent film adhesion was greatly improved with the addition of this silver substitution.

The polypyrrole film was then grown using a solution comprised of anhydrous acetonitrile, tetrabutylammonium tetrafluoroborate electrolyte and pyrrole from solution. Previous work has used both potentiostatic¹⁹⁻²⁰ and galvanostatic^{21,23} methods to control the growth of polypyrrole films. Samples were grown using both voltage and current control and it was determined that current control provided higher quality films. The oxidation-reduction potential required a steady square wave using $275 \mu\text{A}/\text{cm}^2$ current density for 20 minutes on each side in an ambient atmosphere/room temperature setting. The use of 12 cycles provides a 1.2-1.4 μm black smooth film. A current density of less than $200 \mu\text{A}/\text{cm}^2$ did not initiate the oxidation cycle of the pyrrole, while current densities greater than $400 \mu\text{A}/\text{cm}^2$ resulted in heavy nucleation on the surface forming polymer growth that was dendritic with high surface roughness, and varying in thickness.

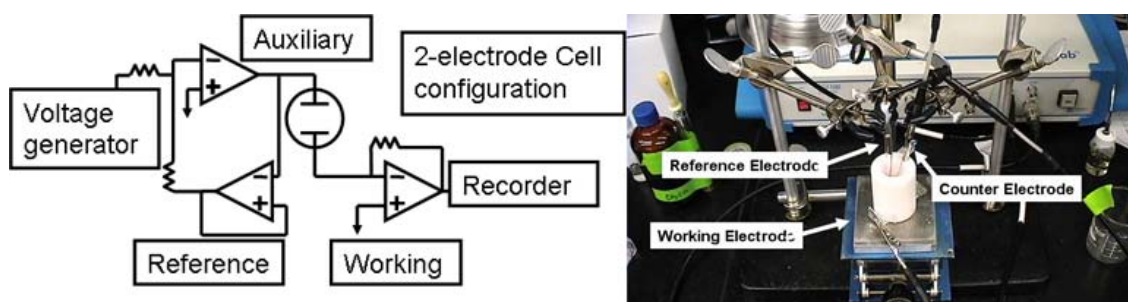


Figure 5. Schematic and original electrochemical cell built for polymer growth on silicon substrates. A larger cell was built for use with 2" substrates.

Conductivities measured on the PPy films ranged from 10-100 S/cm. The adhesion of the film to the substrate was adequate for subsequent processing, but the film could be removed with tape. Also, the film was not removed by photoresist developer allowing for the application and patterning of photoresist without the need for a protective overcoat.

4. PHOTOLITHOGRAPHIC DEVICE FABRICATION

In addition to the need for high conductivity, the device analysis shown in the Section 2 highlighted the thickness and grating dimension that was required for a polarizer with a good extinction ratio. That analysis assumed the grating period used for the gold device (to provide a direct comparison); however, subsequent analysis showed that much larger grating periods could also be used. Assuming a wavelength of $3.39 \mu\text{m}$, grating periods as large as $1.8 \mu\text{m}$ could be used to provide an effective polarizer. This reduced the aspect ratio of the required polymer lines in the final grating and allowed for the use of contact print lithography to pattern the polymer. Additionally, the thickness requirement would necessitate the use of a hard etch mask, so initial efforts were made to process and pattern thinner polymer films of approximately $1 \mu\text{m}$ thickness.

Contact printing patterned the polymer film with grating periods as small as $1.2\ \mu\text{m}$ ($0.6\ \mu\text{m}$ lines). Photoresist was spin coated directly over the polymer film. A standard soft bake, exposure and develop process was used to pattern the photoresist. A UV cure was then substituted for the hard bake typically done after development. This process alteration avoided problems encountered with the polymer reflowing and provided a functional etch selectivity (approximately 1:1). A reactive ion etch (RIE) was then used to transfer the pattern into the polymer¹⁷ using an oxygen based etch recipe, see Figure 6.

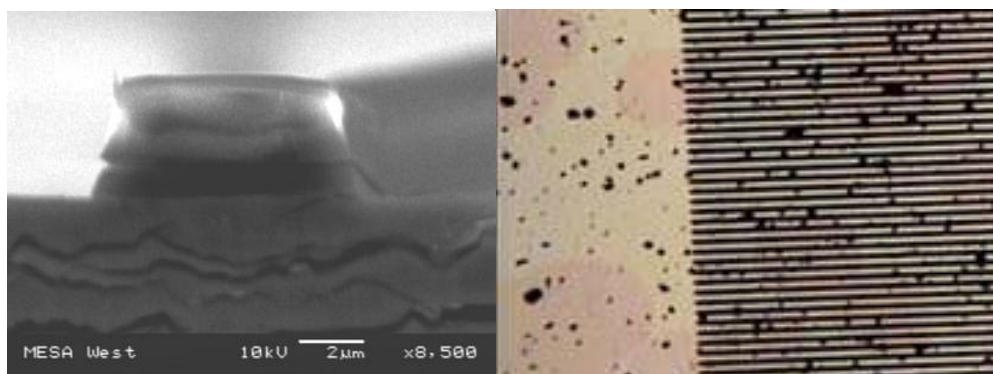


Figure 6. Successfully patterned PPy films. Test etch of a relatively large feature ($8\ \mu\text{m}$) using thick photoresist (left) and image of patterned $0.6\ \mu\text{m}$ lines in polymer (right).

The final fabrication process is the removal of the polymer grating from the seed metal. As mentioned earlier, the polymer film could be removed from the substrate with tape. Patterned polymer was also easily removed using tape so a transfer process was investigated for lifting the polymer lines off the original substrate. In order for the device to be practical at the design wavelength of $3.39\ \mu\text{m}$, the material used to lift off the polymer had to be transmissive. Most tapes and adhesives do not transmit well in the IR, but we found that Norland 61™ optical adhesive would allow a substantial amount of transmission if spin coated. The Norland adhesive was spin coated directly on to the patterned polymer and cured. Using samples grown on Ti/Au, a diluted hydrofluoric acid etch lifted off the adhesive layer and polymer. Similarly, a buffered oxide etch also successfully lifted off the adhesive backed polymer from the original substrate. These flexible devices could then be put on a hard substrate to facilitate optical testing. A SEM image of a transferred grating is shown in Figure 7.

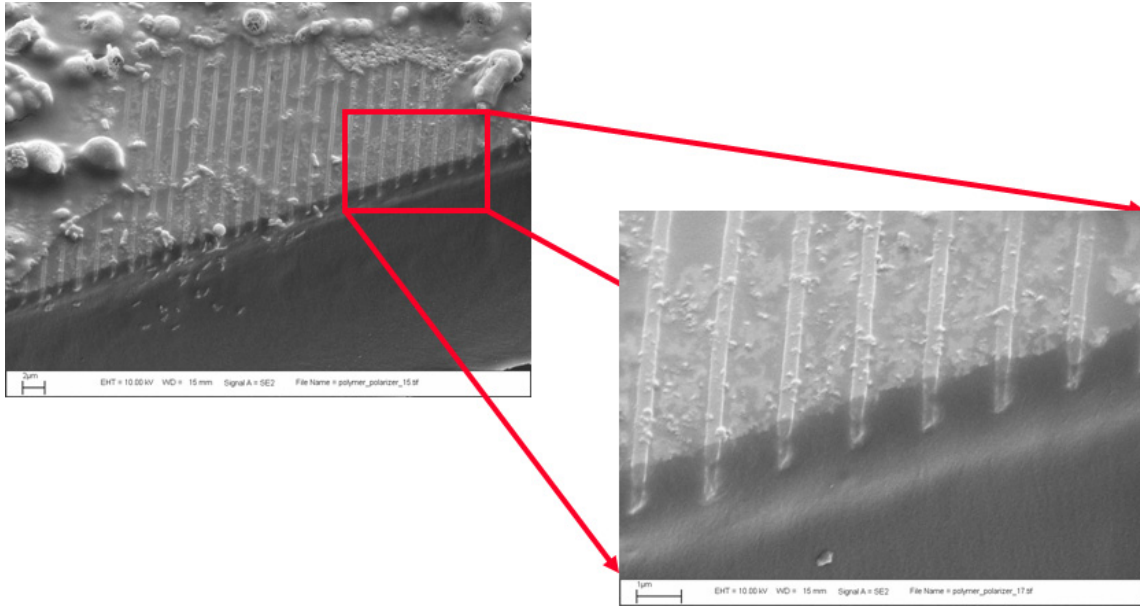


Figure 7. SEM image of transferred polymer grating embedded in Norland 61™. Grating period is 1.6 μm

One characteristic that is clear in Figure 7 is the small duty cycle of the grating. The design assumed a 50% duty cycle; however, the fabricated gratings have typically exhibited duty cycles of approximately 20%. The reason for this reduced duty cycle was determined to be the presence of isotropic reactive etching within the RIE leading to an undercutting of the photoresist used as the etch mask. A new mask with biased lines was used in the latter stages of the project and resulted in improved linewidths in the final devices. Figure 8 below shows wafers and devices at three steps of the process: after photoresist patterning, after etching and after device transfer.

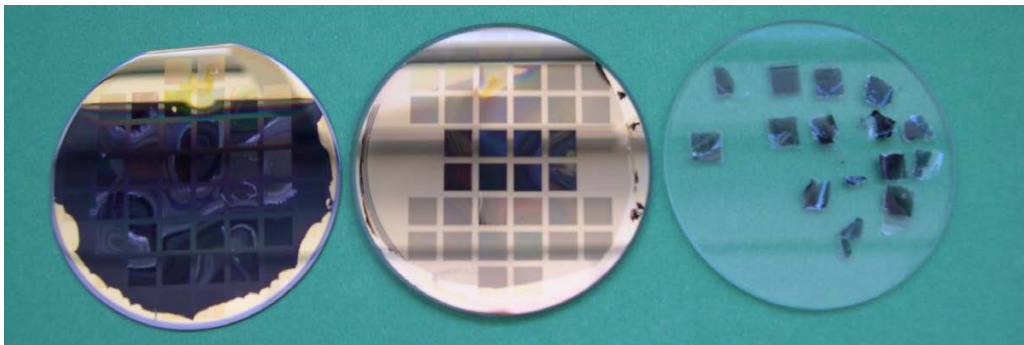


Figure 8. Wafers showing (left to right) patterned photoresist, etched devices and transferred devices.

5. OPTICAL DEVICE CHARACTERIZATION

Several devices were tested optically and even 1.0 μm thick polymer provided measurable modulation of a polarized beam. A HeNe laser emitting at 3.39 μm was used as the input source with a specified linear polarization of 500:1. A half wave plate provided a convenient means of rotating the input linear polarization to the device under test (DUT). The transmitted signal was then detected using a HgCdTe detector. A chopper placed at the laser was used to synchronize a

lock-in amplifier and eliminate background noise providing a high signal to noise ratio (SNR). Figure 9 shows the optical test setup used to characterize the devices. The signal was recorded as the half wave plate was rotated through one full rotation. A background measurement was also taken without the DUT in place to take into account any diattenuation and beam drift caused by the rotating wave plate. The data from these measurements was used in conjunction with the physical parameters of the grating to determine the complex refractive index of the conductive polymer. By iterating with rigorous coupled wave analysis (RCWA), the polymer's material properties were found.



Figure 9. Optical test setup for characterizing optical devices. HeNe laser is on left with chopper. Rotating waveplate is in square mount in front of monitor detector. Sample holder is on left directly in front of cooled HgCdTe detector (red dewar).

The first device measured had patterned polymer wiregrids on top of the metal seed layer. Despite the high loss associated with the metal layers, the high SNR of the test setup allowed for consistent data to be taken. A portion of the gold was removed during the RIE etch as depicted in Figure 10. Figure 10 shows the sample data from a device with a period of $1.2 \mu\text{m}$ as well as the fit determined from RCWA. The resulting refractive index for the polymer was $0.95 - 0.3i$ which corresponds to a conductivity of 28.1 S/cm .

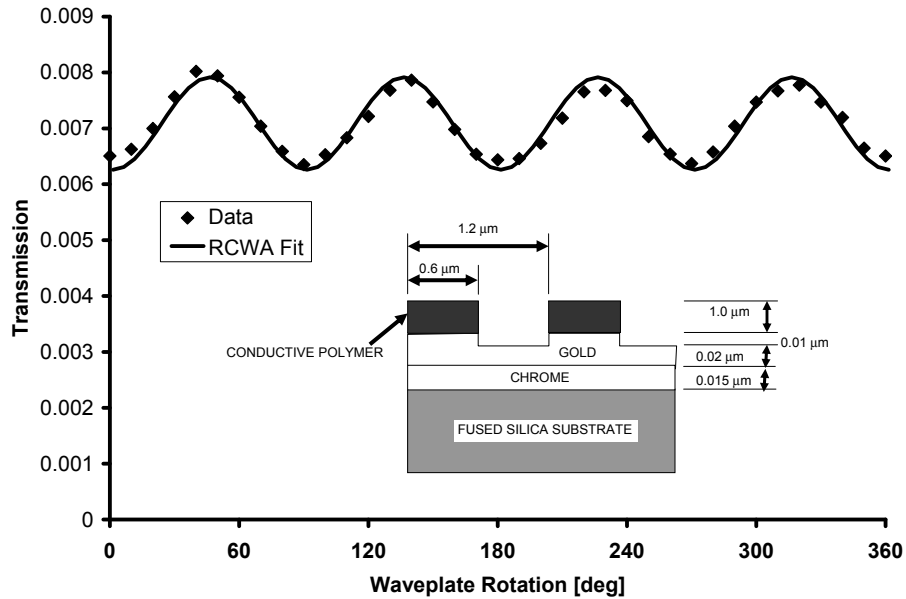


Figure 10. Measured transmission of conductive polymer wire grid (dots) and simulated fit (solid line). The physical parameters are shown on the included diagram.

The final device tested had polymer grown on a titanium/gold seed layer and was removed using diluted hydrofluoric acid that etched the titanium. As mentioned in the previous section, spin coated Norland adhesive was used to pull the gratings off of the original substrate. To ensure mechanical robustness of the adhesive layer, the spin coated layer was relatively thick, approximately 10 μm . The thick adhesive layer resulted in a large loss at the test wavelength of 3.39 μm , but this effect was measured separately and taken into account in the analysis of the DUT. This device also exhibited modulation similar to the original device and had overall higher transmission. Iterative analysis with RCWA showed the polymer to have a complex refractive index of $1.1 - 0.5i$ and a conductivity of 54.2 S/cm. Figure 11 shows the data and simulated fit.

The two measured conductivities are consistent with measurements taken on the polymer films before photolithographic processing. Previous work^{12,15} has shown that some processes can be detrimental to the level of conductivity in the polymer. In fact, a device grown on chrome/gold was tested after the metal layers in the grating trenches were wet-etched. This device exhibited no discernible modulation and our conclusion is that the highly oxidizing chrome etchant (a solution of perchloric acid and ceric ammonium nitrate) effectively destroyed the polymer's conductivity. In light of this type of difficulty, measuring conductivities higher than 50 S/cm in a final device is a very encouraging result.

6. IONIZING RADIATION SENSITIVITY

While the development of the optical polarizer has proceeded, the characterization of the conducting polymer's sensitivity to ionizing radiation has begun. The analysis shown earlier assumed that ionizing radiation would produce a decrease in the conductivity of the polymer. Previous work on polyaniline irradiated with both high and low energy protons did show a

measurable decrease in conductivity^{24,25}. Additionally, gamma ray and electron beam irradiation have produced conductivity decreases^{26,27}. Unfortunately, there are also reports showing the opposite result. Gamma ray irradiation was shown to produce increased conductivity in polyaniline²⁸ as was heavy ion irradiation in conducting polypyrrole²⁹ and polythiophene³⁰. In light of these apparently contradictory results, it is imperative that the material being used here be studied experimentally.

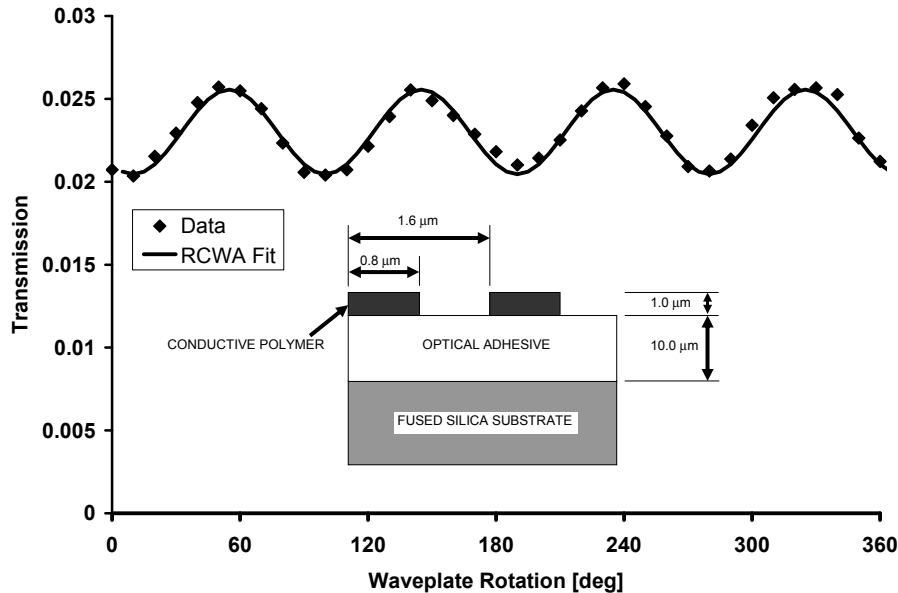


Figure 11. Measured data (dots) and simulated transmission (solid line) of polymer wire grid transferred via optical adhesive

Fortunately, the direction of change in conductivity is not as important as the degree of change. A device that is non-polarizing and then becomes polarizing after being irradiated is still an effective device for this application. However, the magnitude of the conductivity change must be significant enough to produce a measurable change in the optical polarizer's performance. Again, this point highlights the need to experimentally characterize the material being developed.

Our first experiments have used protons with an energy of 250 keV in an evacuated chamber. Figure 12 shows the effect of this irradiation on the conductivity of the polymer. At large total doses (5Mrad or greater) the conductivity of the material is almost completely destroyed (>95% reduction). This result is consistent with published results using low energy irradiation²⁵⁻²⁷. At lower doses, an increase in the material conductivity can be seen before the trend reverses. This may be due to the ionizing radiation acting as a catalyst allowing excess dopant to attach to the polymer chain and enhance the total material conductivity. As the dose increases, damage to the polymer chains becomes the dominant result of the exposure to the protons leading to the ultimate decrease of conductivity.

The first experiments were done using a standard four point probe measurement of the polymer conductivity. This was problematic due to the tendency of the probes to break completely through the thin polymer layer. In addition, we speculate that micro-cracking in the polymer due to handling of the samples might render the four point probe ineffective in measuring the

polymer's conductivity. For lower doses, these difficulties led to large variations from one experiment to another. As an alternative, ellipsometry measurements were used to determine the optical properties of the material. Figure 12 shows data taken using both four point probe measurements (doses > 1 Mrad) and ellipsometry based measurements (doses < 1 Mrad).

The solid line shows an approximate fit to the data after the catalytic effects of the ionizing radiation have been surpassed. Using this relationship, a model of the signal contrast with respect to polarization can be formulated. This would be the measured characteristic used to determine the total dose the device has received. Combining the RCWA results, Figure 3, with the radiation sensitivity shown in Figure 12, the expected relationship between contrast and total dose is shown in Figure 13. Contrast is defined as:

$$Contrast = \frac{TM - TE}{TM + TE} \quad (2)$$

Where TM is the transmitted TM signal and TE is the transmitted TE signal.

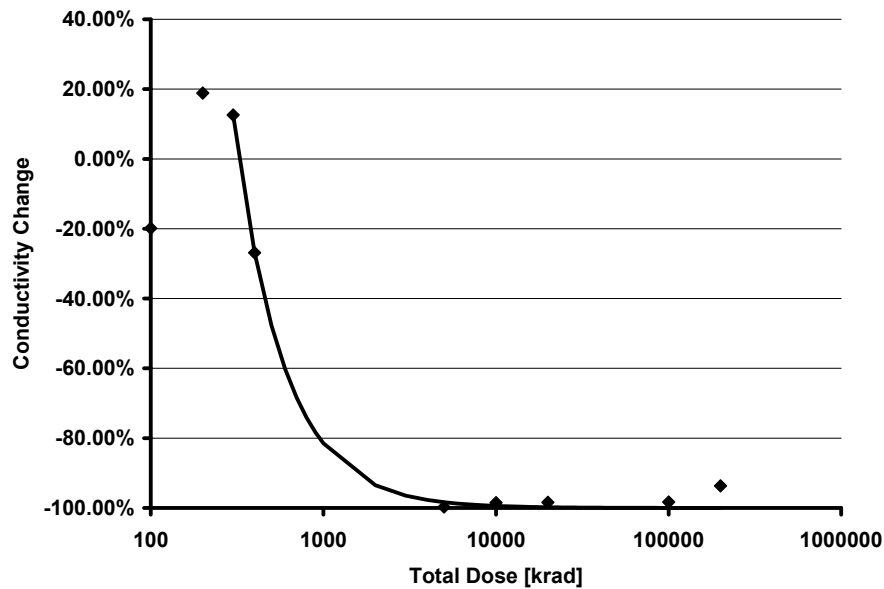


Figure 12. Change of polymer conductivity with total dose. Results below 1Mrad taken using ellipsometry. Results above 1 Mrad measured using four-point probe.

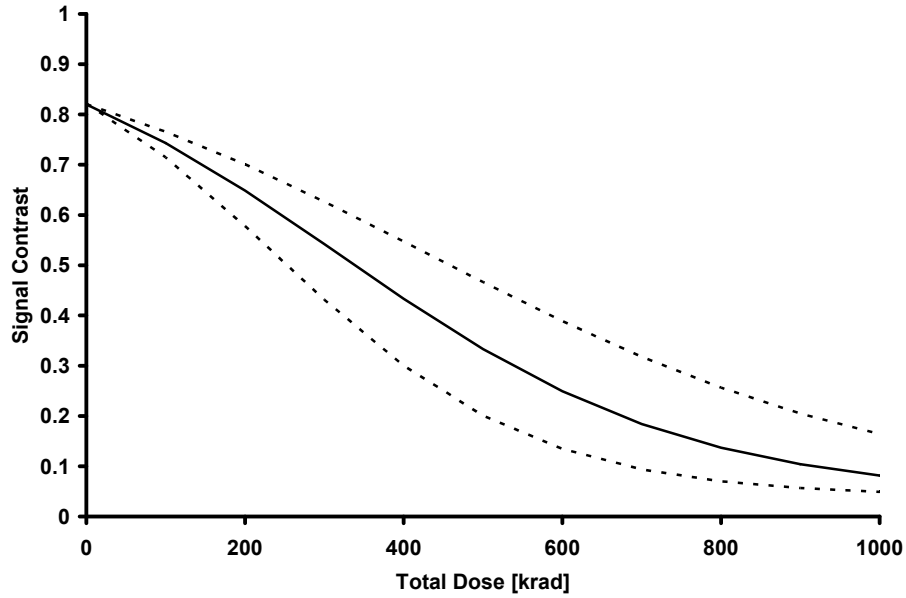


Figure 13. Modeled change in signal contrast of polymer polarizer based tag with respect to total absorbed dose. Dotted lines denote effect of +/- 20% change in sensitivity of polymer.

Originally, we endeavored to determine a transfer curve similar to Figure 13 empirically. While we did not achieve this final goal, we did characterize several devices before and after irradiation and an example result is shown in Figure 14. The measured optical response was adversely effected by the exposure to the protons.

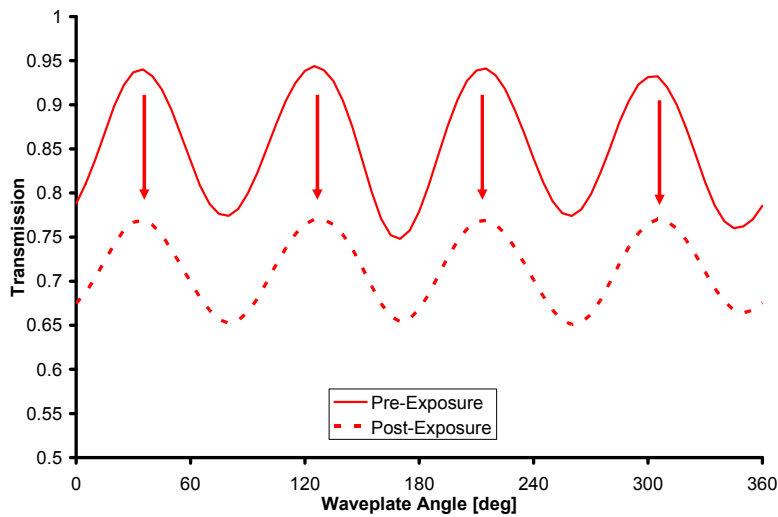


Figure 14. Optical response of device before and after exposure to 250keV protons with a total dose of 400 krad. Note that the contrast of the original signal is not as high as desired due to reduced thickness of polymer and duty cycle of grating similar to results shown in Figure 7.

7. CONCLUSIONS AND FUTURE WORK

The concept of an optical polarizer susceptible to ionizing radiation as a passive dosimeter has been presented. The background of optical wiregrid polarizers and the use of conducting polymers in their design has been reviewed with the tradeoff of device extinction ratio and transmission highlighted. Our progress in both the development of conducting polypyrrole has led to the demonstration of uniform film thicknesses greater than 1.0 μm with conductivities reaching 100 S/cm. The fabrication of wiregrid devices using this material has successfully produced gratings with features as small as 600 nm and these devices have been characterized optically. Finally, the results from the first tests of the polymer's sensitivity to proton irradiation have been shown to have a significant effect on the conductivity of the material.

There are several tasks that are now being pursued as part of this program. First, thicker polymer films are being deposited to provide optical polarizers with usable extinction ratios. Film thicknesses of greater than 2.0 μm have already been made. The need for better control of the duty cycle of the final devices is also being pursued as well as an improved transfer process for removing the gratings from the metal seed layer. The characterization of the polymer to ionizing radiation is also continuing as we experimentally verify the optical device performance expected from the conductivity measurements made thus far. We will also be characterizing the material with other types of radiation to see if radiation type and / or dose rate are also factors in the effects on conductivity.

8. REFERENCES

1. Gang Yu, Jian Wang, Jon McElvain and Alan J. Heeger, "Large-Area, Full-Color Image Sensors Made with Semiconducting Polymers," *Adv. Mat.*, vol. 10 (1998) pp. 1474-1477.
2. Evan L. Williams, Ghassan E. Jabbour, Qi Wang, Sean E. Shaheen, David S. Ginley and Eric A. Schiff, "Conducting polymer and hydrogenated amorphous silicon hybrid solar cells," *Appl. Phys. Lett.*, vol. 87, no. 22 (2005).
3. G.E. Jabbour, D.L. Mathine, B. Kippelen and N. Peyghambarian, "Micro-pixel arrays of bright organic electroluminescent devices for high definition displays," *Elec. Lett.*, vol. 33, no. 24 (20-Nov-97) pp. 2070-2071.
4. Peter K.H. Ho, Ji-Seon Kim, Jeremy H. Burroughes, Heinrich Becker, Sam F.Y. Li, Thomas M. Brown, Franco Cacialli and Richard H. Friend, "Molecular-scale interface engineering for polymer light-emitting diodes," *Nature*, vol. 404 (30-Mar-2000) pp. 481-484.
5. Evan L. Williams, Jian Li and Ghassan E. Jabbour, "Organic light-emitting diodes having exclusive near-infrared electrophosphorescence," *Appl. Phys. Lett.*, vol. 89, no. 8 (2006).
6. A.A. Cruz-Cabrera, S.A. Kemme, J.R. Wendt, R.R. Boye, T.R. Carter and S. Samora, "Edge Termination Effects on Finite Aperture Polarizers for Polarimetric Imaging Applications at Mid Wave IR," *Proc. SPIE*, vol. 6126 (2006).
7. G.P. Nordin, J. T. Meier, P. C. Deguzman and M. W. Jones, "Micropolarizer array for infrared imaging polarimetry," *J. Opt. Soc. Am. A.*, vol. 16, no. 5 (May 1999) pp. 1168-1174.

8. J. Guo and D. J. Brady, "Fabrication of high-resolution micropolarizer arrays," *Opt. Eng.*, vol. 36, (1997) pp. 2268-2271.
9. Serge N. Vinogradov and Robert H. Linnell, "The System Pyridine-Pyrrole and the Association of Pyrrole," *Jour. Chem. Phys.*, vol. 23, no. 1 (Jan. 1955) pp. 93-97.
10. Jing Zhang, Mei Zhen Wu, Tian Shu Pu, Zheng Yang Zhang, Ruo Peng Jin, Zhi Shen Tong, De Zhang Zhu, De Xin Cao, Fu Ying Zhu, Jian Qing Cao, "Investigation of the plasm polymer deposited from pyrrole," *Thin Solid Films*, vol. 307 (1997) pp. 14-20.
11. Joachim Bargon and Reinhard Baumann, "Laser-induced generation and patterning of electrically conducting polymers," *Proc. SPIE*, vol. 1910 (1993) pp. 92-100.
12. Teresita Graham, Marie Angelopoulos, Bruce Furman, Rex Chen and Wayne Moreau, "Conducting polyaniline coatings for submicron lithography and SEM metrology," *Proc. SPIE*, vol. 3048 (1997) pp. 105-113.
13. M. Born and E. Wolf, *Principles of Optics*, Pergamon, New York (1980).
14. Maggie A.Z. Hupcey, Marie Angelopoulos, Jeffrey D. Gelorme and Christopher K. Ober, "Conducting Electron Beam Resists Based on Polyaniline," *Proc. SPIE*, vol. 3331 (1998) pp. 369-374.
15. Teresita Graham, Ali Afzali, Marie Angelopoulos, Jeffrey Gelorme and Jane Shaw, "Patterning of Highly Conducting Polyaniline Films," *Proc. SPIE*, vol. 3997 (2000) pp. 334-343.
16. Hitoshi Koizumi, Hiroshi Dougauchi, Tadaomi Yamano and Tsuneki Ichikawa, "Mechanism of Radiation-Induced Doping," *Jpn. J. Appl. Phys.*, vol. 42 (2003) pp. 7122-7123.
17. C. Nilsson, E.H. Karlsson and H. Kariis, "Polymer based devices with adaptable infrared reflection and transmission," *Proc. SPIE*, vol. 6192 (2006) pp. 61921U1 – 8.
18. H.C. Stark "Baytron P" Product Data Sheet.
19. Elisabeth Smela, Matthias Kallenbach and Jens Holdenried, "Electrochemically Driven Polypyrrole Bilayers for Moving and Positioning Bulk Micromachined Silicon Plates," *Jour. MicroElecMech Syst.*, vol. 8, no. 4 (Dec. 1999) pp. 373-383.
20. Myoungcho Pyo, Clayton C. Bohn, Elisabeth Smela, John R. Reynolds and Anthony B. Brennan, "Direct Strain Measurement of Polypyrrole Actuators Controlled by the Polymer/Gold Interface," *Chem. Mater.*, vol. 15 (2003) pp. 916-922.
21. Carlos Cesar Bof Bufon, Judith Vollmer, Thomas Heinzl, Pamela Espindola, Hermann John and Jürgen Heinze, "Relationship between Chain Length, Disorder, and Resistivity in Polypyrrole Films," *J. Phys. Chem. B*, vol. 109 (2005) pp. 19191-19199.
22. Yu-Chuan Liu, "Modification of Electrochemically Roughened Au(111) by Underpotentially Deposited Silver and Its Effect on the Subsequent Electrodeposition of Polypyrrole," *Langmuir*, vol. 19 (2003) pp. 6888-6893.
23. Farid A. Harraz, "Electrochemical Polymerization of Pyrrole into Nanostructured p-Type Porous Silicon," *Jour. Electrochem. Soc.*, vol. 153, no. 5 (2006) pp. C349-C356.
24. Qi Yao, Limin Liu and Changjiang Li, "High Energy Proton Beam Bombardment of Polyaniline," *Radiat. Phys. Chem.*, vol. 41, no. 6 (1993) pp. 791-795.
25. Qi Yao, Limin Liu and Changjiang Li, "Low Energy Proton Implanted Polyaniline," *Radiat. Phys. Chem.*, vol. 44, no. 4 (1994) pp. 381-384.
26. M. Wolszczak, J. Kroh and M.M. Abdel-Hamid, "Some aspects of the radiation processing of conducting polymers," *Radiat. Phys. Chem.*, vol. 45, no. 1 (1995) pp. 71-78.

27. W.M. de Azevedo, A.P. da Costa Lima and E.S. de Araujo, "Radiation-induced effects on electrical properties of polyaniline," Rad. Protection Dosimetry, vol. 84, nos. 1-4 (1999) pp.77-81.
28. Qi Yao, Limin Liu and Changjiang Li, "Studies on electrical conductivity of gamma irradiated polyaniline," Polymer Bulletin, vol. 31 (1993) pp. 601-605.
29. A.M.P. Hussain, A. Kumar, D. Saikia, F. Singh and D.K. Avasthi, "Study of 160 MeV Ni¹²⁺ ion irradiation effects on electrodeposited polypyrrole films," Nuc. Inst. Meth. B, vol. 240 (2005) pp. 871-880.
30. A. Kumar and A.M.P. Hussain, "120 MeV Si⁹⁺ ion irradiation effects on poly(3-methylthiophene) conducting polymer," Nuc. Inst. Meth. B, vol. 251 (2006) pp. 451-456.

Distribution

5	MS 1082	Robert Boye, 1725
1	MS 1082	Shanalyn Kemme, 1725
1	MS 1082	Jim Hudgens, 1725
1	MS 1210	Jim Novak, 5935
1	MS 0888	Cody Washburn, 1821
1	MS 0888	Shawn Dirk, 1821
1	MS 0892	Dave Wheeler, 1714
1	MS 0406	Prabal Nandy, 5713
1	MS 0899	Technical Library, 9536 (electronic copy)
1	MS 0123	Donna Chavez, LDRD Office, 1011

